ORIGINAL ARTICLE

lajss.org Latin American Journal of Solids and Structures
www.lajss.org

Vibration Analysis of Axially Functionally Graded Timoshenko Beams with Non-uniform Cross-section

Wei-Ren Chen[a*]

[a]Chinese Culture University, Taipei 11114, Taiwan. wrchen@ulive.pccu.edu.tw

* Corresponding author

https://doi.org/10.1590/1679-78256434

Abstract
The present paper investigates the transverse vibration of a non-uniform axially functionally graded Timoshenko beam with cross-sectional and material properties varying in the beam length direction. The Chebyshev collocation method is used to spatially discretize the governing partial differential equations of motion of the beam into time-dependent ordinary differential equations in terms of Chebyshev differentiation matrices. An algebraic eigenvalue equation in matrix form is then formed to study the free vibration behavior of non-uniform axially functionally graded Timoshenko beams. Several results of natural frequencies of the beams are evaluated and compared with those in the published literature to assure the accuracy of the proposed model. The effects of taper ratio, material graded index, slenderness ratio, material compositions and restraint types on the natural frequencies of tapered axially functionally graded Timoshenko beams are examined.

Keywords
axially functionally graded, Chebyshev collocation method, natural frequency, taper ratio

Graphical abstract

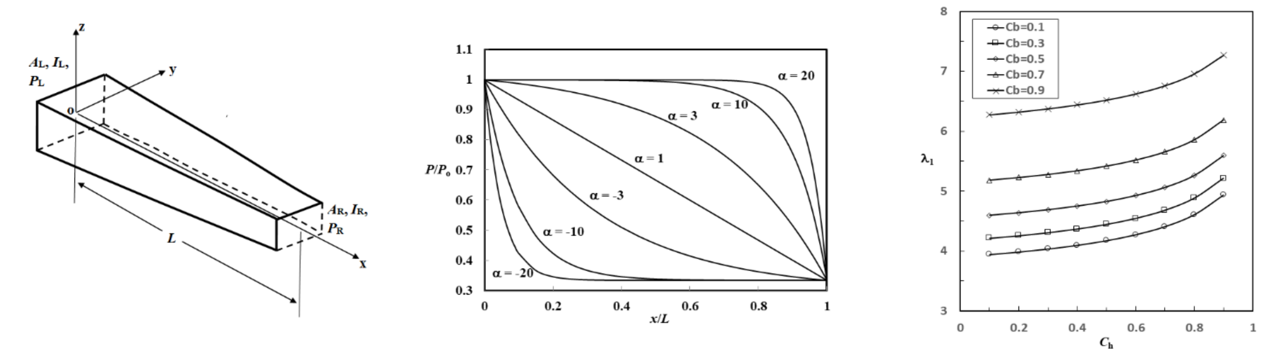

Received February 03, 2021. In revised form August 27, 2021. Accepted September 08, 2021. Available online September 10, 2021.
https://doi.org/10.1590/1679-78256434

1 INTRODUCTION

Functionally graded materials (FGMs) have been used increasingly in various engineering and scientific fields recently because of their promising material properties over the traditional composites. Thus, the dynamic problems of engineering structures constructed from FGMs have received considerable attention, especially for the beam members commonly used in bridges, buildings and machine components. In the past decades, most studies numerically dealt with the dynamics of FGM beams with material properties graded in the thickness direction based on various beam theories (Simsek (2010); Thai and Vo (2012); Nguyen et al. (2013); Pradhan and Chakraverty (2014); Su and Banerjee (2015); Wattanasakulpong and Mao (2015); Chen and Chang (2017, 2018); Ding et al. (2018); Esen (2019)). It is noted that the strength and weight of beam structures, which affect its vibration behavior, can be optimized by changing the cross-sectional and material properties along the beam length direction. Therefore, the dynamic problems of FGM beams with axially varying properties have received considerable attention in recent years.

The free vibration of non-uniform axially FGM Euler-Bernoulli beams with various end supports was presented by Huang and Li (2010) based on the integral equation method. The bending vibration of FGM beams with axial variation of material properties was investigated by Murin et al. (2010). The free vibration and stability of tapered axially FGM Timoshenko beams with various restraint conditions was dealt with by Shahba et al. (2011) by using finite element analysis. The vibration analysis of non-uniform axially FGM beams was presented by Hein and Feklistova (2011) based on the Euler-Bernoulli beam theory and Haar wavelet approach. Based on the lowest-order differential quadrature element and differential transform element methods, the vibration and stability problems of axially FGM Euler–Bernoulli beams with tapered cross-section were investigated by Shahba and Rajasekaran (2012). Exact frequency equations of the free vibration for axially exponentially FGM beams with different end conditions were presented by Li et al. (2013) by employing an analytical approach. The lowest-order differential quadrature element and differential transform element methods were used by Rajasekaran (2013a, 2013b) to analyze the vibration behavior of rotating non-uniform axially FGM Euler–Bernoulli and Timoshenko beams. The free vibration of axially FGM Timoshenko beams with non-uniform cross-section was studied by Huang et al. (2013) based on a unified approach. The free vibration of clamped axially FGM uniform Timoshenko beams was studied by Sarkar and Ganguli (2014). Exact equations of vibration frequencies of tapered axially FGM Timoshenko beams were derived by Tang et al. (2014). The spline finite point method was applied by Liu et al. (2016) to study the free bending vibration of axially FGM beams with tapered cross-section by using the Euler-Bernoulli beam theory. The complementary functions method was used by Calim (2016) to investigate the transient vibration of tapered axially FGM Timoshenko beams. Based on the Euler-Bernoulli and Timoshenko beam theories, the vibration behaviors of non-uniform axially FGM beams were investigated by Zhao et al. (2017) by using the Chebyshev polynomials theory. The asymptotic development method was presented by Cao et al. (2018) to analyze the free vibration of axially FGM Euler-Bernoulli beams. The vibration of tapered axially FGM cantilevered Timoshenko beam under various axial loadings was investigated by Sun and Li (2019) based on the initial value method. The bending vibration of non-uniform axially FGM Euler-Bernoulli beams was investigated by Chen (2020) based on the Chebyshev collocation method.

As reviewed above, the vibration problems of axially FGM beams (AFGM) had been effectively studied by many researchers based on numerous numerical methods. The Chebyshev collocation method has the advantages of fast convergence rate and high accuracy of predictability over other numerical methods so it has been widely used to solve various engineering and mathematical problems. However, there exists a paucity of the contribution of the published literature to the vibration of non-uniform AFGM Timoshenko beams by using the Chebyshev collocation method. Thus, an attempt has been made to apply the Chebyshev collocation method to analyze the transverse vibration of FGM Timoshenko beams with axially varying material and cross-sectional properties. Material properties are assumed to vary along the length direction described by the exponential function. The Chebyshev collocation method is applied to reduce the partial differential equations of motion into the ordinary differential equations with time as the indendent variable. Then, an eigenvalue problem is formulated to evaluate the free vibration behavior of the tapered AFGM Timoshenko beam. The natural frequencies for various AFGM beams with different taper ratios, slenderness ratios, graded indices, material constituents and boundary conditions are determined. In comparing the calculated natural frequencies with those by other investigators, the present results agree well with those obtained by other methods. Then, relevant parameter analyses are performed to demonstrate the effects of various material and geometric parameters on the free vibration characteristics of the AFGM Timoshenko beams.

2 BENDING VIBRATION ANALYSIS

The AFGM beam with tapered rectangular cross-section as shown in Figure 1 is considered. The beam has a length L with taper ratios in the width and thickness directions. The axes x, y and z represent the respective beam length, width and thickness direction. The cross-sectional properties, area $A(x)$ and area moment of inertia $I(x)$, of the tapered beam are assumed to vary along the axial direction as follows.

$$A(x) = A_o\left(1 - C_b\frac{x}{L}\right)\left(1 - C_h\frac{x}{L}\right) \tag{1}$$

$$I(x) = I_o\left(1 - C_b\frac{x}{L}\right)\left(1 - C_h\frac{x}{L}\right)^3 \tag{2}$$

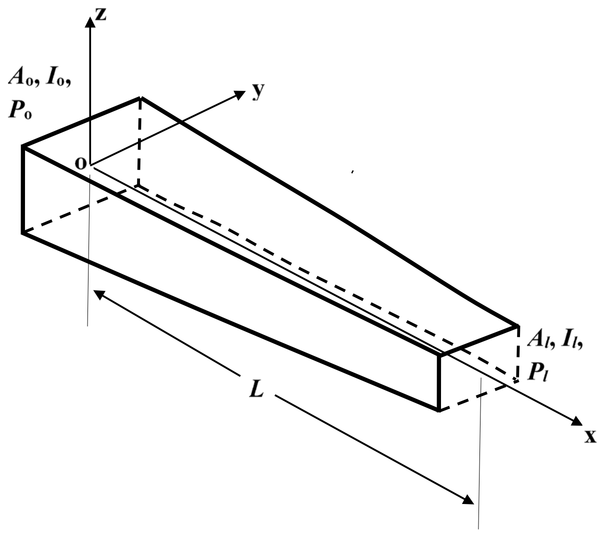

Figure 1: Axially FGM beam configuration and coordinate systems.

Here A_o and I_o are the area and area moment of inertia at the left end $x = 0$; C_b and C_h are the width and height taper ratio, respectively. The material properties, Young's modulus $E(x)$ and shear modulus $G(x)$ and mass density $\rho(x)$, of the AFGM beam are represented by the effective material property $P(x)$, which varies continuously across the beam length according to the following exponential function.

$$P(x) = P_o + (P_l - P_o)\frac{e^{\alpha x/L}-1}{e^{\alpha}-1} \quad \alpha \neq 0. \tag{3a}$$

$$P(x) = P_o + (P_l - P_o)\frac{x}{L} \quad \alpha = 0. \tag{3b}$$

where P_o and P_l are the material properties at the left and right surface of the beam, respectively; The exponent α is the material graded index which describe the material variation profile of the volume fraction through the beam length; the length variable x ranges from 0 to L. Figure 2 depicts the variation of property P/P_o in the length direction for $P_o = 3P_l$. As can be seen, a smaller value of volume fraction index represents a more sudden increase in the property P/P_o near the left surface and the material at the right surface is the dominant constituent. In contrast, the property P/P_o changes abruptly near the right surface for a larger value of volume fraction index and the dominant constituent is the material at the left surface.

By applying Timoshenko beam theory and Hamilton's principle to the non-uniform axially FGM beam, the following partial differential equations (Shahba et al. (2011)) with variable coefficients and boundary conditions governing the lateral free vibration behaviors of AFGM Timoshenko beams can be obtained.

$$\frac{\partial}{\partial x}\left(kG(x)A(x)\left(\frac{\partial w}{\partial x} - \varphi\right)\right) - \rho(x)A(x)\frac{\partial^2 w}{\partial t^2} = 0 \tag{4a}$$

$$\frac{\partial}{\partial x}\left(E(x)I(x)\frac{\partial \varphi}{\partial x}\right) + kG(x)A(x)\left(\frac{\partial w}{\partial x} - \varphi\right) - \rho(x)I(x)\frac{\partial^2 \varphi}{\partial t^2} = 0 \tag{4b}$$

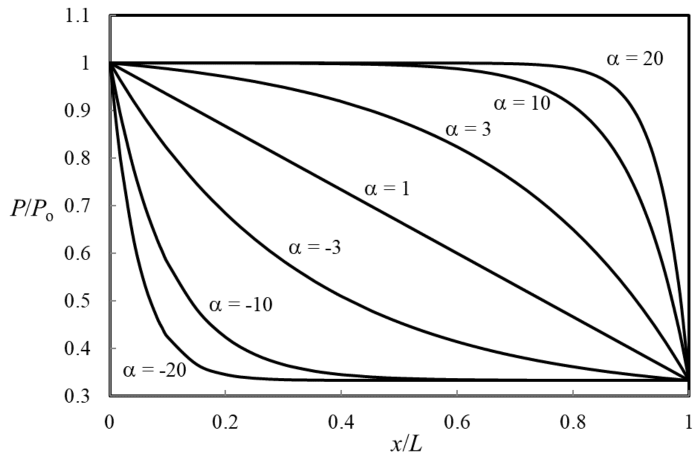

Figure 2: Variation of effective property $P(x)/P_o$ versus beam length for exponentially AFGM beam with various values of material graded index α.

Clamped end: $\mathrm{w} = 0, \varphi = 0$ (5a)

Pinned end: $\mathrm{w} = 0, \frac{\partial \varphi}{\partial \mathrm{x}} = 0$ (5b)

Free end: $\frac{\partial \varphi}{\partial \mathrm{x}} = 0, \frac{\partial \mathrm{w}}{\partial \mathrm{x}} - \varphi = 0$ (5c)

where w is the transverse displacement along the z direction and φ is the rotation about the y axis; κ is the shear correction factor and taken to be 5/6 throughout this paper. The present study intends to use the Chebyshev collocation method to solve the free vibration equations (4) and (5). Because the space variable range of this collocation method is [-1, 1], the space variable must be transformed before analysis. Let $\xi = 2\,x/L - 1$, Eqs. (4) and (5) can be rewritten as the partial differential equations with ξ as the spatial independent variable as follows.

$$m(\xi)\frac{\partial^2 w}{\partial t^2} - \left(\frac{2}{L}\right)^2 Q(\xi)\frac{\partial^2 w}{\partial \xi^2} - \left(\frac{2}{L}\right)^2 Q'(\xi)\frac{\partial w}{\partial \xi} + \left(\frac{2}{L}\right) Q(\xi)\frac{\partial \varphi}{\partial \xi} + \left(\frac{2}{L}\right) Q'(\xi)\varphi = 0 \tag{6a}$$

$$J(\xi)\frac{\partial^2 \varphi}{\partial t^2} - \left(\frac{2}{L}\right)^2 S(\xi)\frac{\partial^2 \varphi}{\partial \xi^2} - \left(\frac{2}{L}\right)^2 S'(\xi)\frac{\partial \varphi}{\partial \xi} + Q(\xi)\varphi - \left(\frac{2}{L}\right) Q(\xi)\frac{\partial w}{\partial \xi} = 0 \tag{6b}$$

Clamped end: $w = 0, \varphi = 0$ (7a)

Pinned end: $w = 0, \frac{\partial \varphi}{\partial \xi} = 0$ (7b)

Free end: $\frac{\partial \varphi}{\partial \xi} = 0, \left(\frac{2}{L}\right)\frac{\partial w}{\partial \xi} - \varphi = 0$ (7c)

where $Q(\xi) = kG(\xi)A(\xi)$ is the shear rigidity; $S(\xi) = E(\xi)I(\xi)$ is the bending rigidity; $m(\xi) = \rho(\xi)A(\xi)$ and $J(\xi) = \rho(\xi)A(\xi)$ are the mass and rotary inertia per unit length, respectively.

Using the Chebyshev collocation method to spatially discretize the partial differential equation (6), and considering the Chebyshev-Gauss-Lobatto (CGL) collocation point, the displacement function $\mathrm{w}(\xi, t)$ and the rotation function $\varphi(\xi, t)$ can be expressed as the following Nth-order Chebyshev polynomial.

$$w(\xi, t) \approx \sum_{j=0}^{N} \gamma_j(\xi) w\left(\xi_j, t\right) \tag{8a}$$

$$\varphi(\xi, t) \approx \sum_{j=0}^{N} \gamma_j(\xi) \varphi\left(\xi_j, t\right) \tag{8b}$$

with

$$\xi_j = cos\left(\frac{\pi j}{N}\right), j = 0, 1, 2 \cdots N \tag{9a}$$

$$\gamma_j(\xi) = \frac{(-1)^{j+1}(1-\xi^2)T_N'(\xi)}{c_j N^2\left(\xi-\xi_j\right)} \tag{9b}$$

$$T_N\left(\xi_j\right) = cos\left(Ncos^{-1}\left(\xi_j\right)\right) \tag{9c}$$

$$\gamma_j\left(\xi_k\right) = \delta_{jk} \tag{9d}$$

$$c_j = \begin{cases} 2 & j = 0, N \\ 1 & j = 1, 2 \cdots N-1 \end{cases} \tag{9e}$$

Here ξ_j are the Gauss-Chebyshev-Lobatto collocation points (Trefethen, 2000) within [-1, 1]. Then, the matrix vector multiplication is used to obtain the first derivatives of the displacement functions in Eq. (8) at the collocation points as

$$w'\left(\xi_i, t\right) = \sum_{j=0}^{N}(D_N)_{ij} w\left(\xi_j, t\right), i = 0, 1, 2 \cdots N \tag{10a}$$

$$\varphi'\left(\xi_i, t\right) = \sum_{j=0}^{N}(D_N)_{ij} \varphi\left(\xi_j, t\right), i = 0, 1, 2 \cdots N \tag{10b}$$

where D_N denotes the (N+1)×(N+1) Chebyshev differentiation matrix; $(D_N)_{ij}$ is its entry at row *i* and column *j*, which is given as (Trefethen, 2000)

$$(D_N)_{00} = \frac{2N^2+1}{6}, \quad (D_N)_{NN} = -\frac{2N^2+1}{6} \tag{11a}$$

$$(D_N)_{jj} = -\frac{\xi_j}{2\left(1-\xi_j^2\right)}, j = 1,2 \cdots N-1 \tag{11b}$$

$$(D_N)_{ij} = \frac{c_i}{c_j}\frac{(-1)^{i+j}}{\left(\xi_i-\xi_j\right)}, i \neq j \; j = 1,2 \cdots N-1 \tag{11c}$$

Eq. (11) represents each element of the first derivative $\boldsymbol{D}_1$ of the Chebyshev differential matrix, and the kth derivative can be obtained by $\boldsymbol{D}_k=(\boldsymbol{D}_1)^k$. It is worth pointing out that although the Chebyshev collocation method has the advantage of providing accurate and fast convergent solutions, it tends to cause physical false eigenvalues, and usually produces more roundoff errors when calculating derivatives. A detailed discussion of spurious unstable modes and roundoff errors in derivative calculations can be found in the books of Gottlieb and Orszag [1977] and Boyd [2000]. Using the above-mentioned Chebyshev collocation method, the partial differential equation (6) can be rewritten into a time-dependent ordinary differential equation represented by the Chebyshev differential matrix.

$$\begin{bmatrix} \overline{\boldsymbol{m}} & \boldsymbol{O} \\ O & \bar{\mathbf{J}} \end{bmatrix} \ddot{\boldsymbol{U}}(t) + \begin{bmatrix} \boldsymbol{K}_{11} & \boldsymbol{K}_{12} \\ \boldsymbol{K}_{21} & \boldsymbol{K}_{22} \end{bmatrix} \boldsymbol{U}(t) = 0 \tag{12}$$

where

$$\boldsymbol{U}(t) = \left\{w_1(t) \quad w_2(t) \quad \cdots \quad w_{N+1}(t) \quad \varphi_1(t) \quad \varphi_2(t) \quad \cdots \quad \varphi_{N+1}(t)\right\}^T$$

$$\ddot{\boldsymbol{U}}(t) = \left\{\ddot{w}_1(t) \quad \ddot{w}_2(t) \quad \cdots \quad \ddot{w}_{N+1}(t) \quad \ddot{\varphi}_1(t) \quad \ddot{\varphi}_2(t) \quad \cdots \quad \ddot{\varphi}_{N+1}(t)\right\}^T$$

$$\boldsymbol{K}_{11} = -\left(\frac{2}{L}\right)^2 \boldsymbol{K}_{s1}\boldsymbol{D}_2 - \left(\frac{2}{L}\right)^2 \boldsymbol{K}_{s2}\boldsymbol{D}_1, \boldsymbol{K}_{12} = \frac{2}{L}\boldsymbol{K}_{s1}\boldsymbol{D}_1 + \frac{2}{L}\boldsymbol{K}_{s2}$$

$$\boldsymbol{K}_{21} = -\frac{2}{L}\boldsymbol{D}_1, \boldsymbol{K}_{22} = -\left(\frac{2}{L}\right)^2 \boldsymbol{K}_{b1}\boldsymbol{D}_2 - \left(\frac{2}{L}\right)^2 \boldsymbol{K}_{b2}\boldsymbol{D}_1 + \boldsymbol{K}_{s1}$$

$$\overline{\boldsymbol{m}} = \begin{bmatrix} m(\xi_0) & 0 & \cdots & 0 \\ 0 & m(\xi_1) & \cdots & 0 \\ \vdots & \vdots & \ddots & \vdots \\ 0 & 0 & \cdots & m(\xi_N) \end{bmatrix}, \overline{\boldsymbol{J}} = \begin{bmatrix} J(\xi_0) & 0 & \cdots & 0 \\ 0 & J(\xi_1) & \cdots & 0 \\ \vdots & \vdots & \ddots & \vdots \\ 0 & 0 & \cdots & J(\xi_N) \end{bmatrix}$$

$$\boldsymbol{K}_{s1} = \begin{bmatrix} Q(\xi_0) & 0 & \cdots & 0 \\ 0 & Q(\xi_1) & \cdots & 0 \\ \vdots & \vdots & \ddots & \vdots \\ 0 & 0 & \cdots & Q(\xi_N) \end{bmatrix}, \boldsymbol{K}_{s2} = \begin{bmatrix} Q'(\xi_0) & 0 & \cdots & 0 \\ 0 & Q'(\xi_1) & \cdots & 0 \\ \vdots & \vdots & \ddots & \vdots \\ 0 & 0 & \cdots & Q'(\xi_N) \end{bmatrix},$$

$$\boldsymbol{K}_{b1} = \begin{bmatrix} S(\xi_0) & 0 & \cdots & 0 \\ 0 & S(\xi_1) & \cdots & 0 \\ \vdots & \vdots & \ddots & \vdots \\ 0 & 0 & \cdots & S(\xi_N) \end{bmatrix}, \boldsymbol{K}_{b2} = \begin{bmatrix} S'(\xi_0) & 0 & \cdots & 0 \\ 0 & S'(\xi_1) & \cdots & 0 \\ \vdots & \vdots & \ddots & \vdots \\ 0 & 0 & \cdots & S'(\xi_N) \end{bmatrix},$$

Here $\boldsymbol{U}(t)$ and $\ddot{\boldsymbol{U}}(t)$ are the transpose displacement and acceleration vectors, respectively. Matrices $\overline{\boldsymbol{m}}$, $\overline{\boldsymbol{J}}$, $\boldsymbol{K}_{s1}$, $\boldsymbol{K}_{s2}$, $\boldsymbol{K}_{b1}$ and $\boldsymbol{K}_{b2}$ are all diagonal matrices with diagonal elements formed by evaluating $m(\xi)$, $J(\xi)$, $Q(\xi)$, $Q'(\xi)$, $S(\xi)$ and $S'(\xi)$ at the collocation points, respectively. Similarly, the boundary conditions of the beam as described in Eq. (7) can be expressed in terms of Chebyshev differentiation matrices as shown in Table 1. By imposing the homogeneous boundary conditions at the supporting ends on the governing equation (12) and rearranging the displacement and acceleration vector $\boldsymbol{U}(t)$ and $\ddot{\boldsymbol{U}}(t)$, Eq. (12) is reformulated as

$$\begin{bmatrix} \boldsymbol{O} & \boldsymbol{O} \\ \boldsymbol{M}_{IB} & \boldsymbol{M}_{II} \end{bmatrix} \begin{Bmatrix} \ddot{\boldsymbol{U}}_B(t) \\ \ddot{\boldsymbol{U}}_I(t) \end{Bmatrix} + \begin{bmatrix} \boldsymbol{K}_{BB} & \boldsymbol{K}_{BI} \\ \boldsymbol{K}_{IB} & \boldsymbol{K}_{II} \end{bmatrix} \begin{Bmatrix} \boldsymbol{U}_B(t) \\ \boldsymbol{U}_I(t) \end{Bmatrix} = \mathrm{O} \tag{13}$$

$$\boldsymbol{U}_B(t) = \{w_1(t) \quad w_{N+1}(t) \quad \varphi_1(t) \quad \varphi_{N+1}(t)\}^T$$

$$\boldsymbol{U}_I(t) = \{w_2(t) \quad w_3(t) \quad \cdots \quad w_N(t) \quad \varphi_2(t) \quad \varphi_3(t) \quad \cdots \quad \varphi_N(t)\}^T$$

Table 1 Boundary condition equations in terms of Chebyshev differentiation matrices.

beam	Boundary condition: Left end ($\xi = -1$)	Boundary condition: Right end ($\xi = +1$)
CF	$[1 \quad 0] \otimes [0 \quad 0 \quad \cdots \quad 1]\boldsymbol{U} = \boldsymbol{0}$ $[0 \quad 1] \otimes [0 \quad 0 \quad \cdots \quad 1]\boldsymbol{U} = \boldsymbol{0}$	$[0 \quad 1] \otimes \boldsymbol{D}_1[1, \quad :]\boldsymbol{U} = \boldsymbol{0}$ $\left\{\frac{2}{L}[1 \quad 0] \otimes \boldsymbol{D}_1[1, \quad :] - [0 \quad 1] \otimes [1 \quad 0 \quad \cdots \quad 0]\right\}\boldsymbol{U} = 0$
CP	$[1 \quad 0] \otimes [0 \quad 0 \quad \cdots \quad 1]\boldsymbol{U} = \boldsymbol{0}$ $[0 \quad 1] \otimes [0 \quad 0 \quad \cdots \quad 1]\boldsymbol{U} = \boldsymbol{0}$	$[1 \quad 0] \otimes [1 \quad 0 \quad \cdots \quad 0]\boldsymbol{U} = \boldsymbol{0}$ $[0 \quad 1] \otimes \boldsymbol{D}_1[1, \quad :]\boldsymbol{U} = \boldsymbol{0}$
CC	$[1 \quad 0] \otimes [0 \quad 0 \quad \cdots \quad 1]\boldsymbol{U} = \boldsymbol{0}$ $[0 \quad 1] \otimes [0 \quad 0 \quad \cdots \quad 1]\boldsymbol{U} = \boldsymbol{0}$	$[1 \quad 0] \otimes [1 \quad 0 \quad \cdots \quad 0]\boldsymbol{U} = \boldsymbol{0}$ $[0 \quad 1] \otimes [1 \quad 0 \quad \cdots \quad 0]\boldsymbol{U} = \boldsymbol{0}$
PP	$[1 \quad 0] \otimes [0 \quad 0 \quad \cdots \quad 1]\boldsymbol{U} = \boldsymbol{0}$ $[0 \quad 1] \otimes \boldsymbol{D}_1[N+1, \quad :]\boldsymbol{U} = \boldsymbol{0}$	$[1 \quad 0] \otimes [1 \quad 0 \quad \cdots \quad 0]\boldsymbol{U} = \boldsymbol{0}$ $[0 \quad 1] \otimes \boldsymbol{D}_1[1, \quad :]\boldsymbol{U} = \boldsymbol{0}$

The subscripts 'I' and 'B' are the collocation points related to the respective governing equation and boundary condition. Considering the harmonic vibration, the displacement functions in Eq. (13) are assumed to be

$$\boldsymbol{U}_B(t) = \overline{\boldsymbol{U}}_B e^{i\omega t}; \boldsymbol{U}_I(t) = \overline{\boldsymbol{U}}_I e^{i\omega t} \tag{14}$$

where ω is the natural frequency. Substituting Eq. (14) into Eq. (13), the following algebraic eigenvalue equation is obtained

$$\begin{bmatrix} \boldsymbol{K}_{BB} & \boldsymbol{K}_{BI} \\ \boldsymbol{K}_{IB} & \boldsymbol{K}_{II} \end{bmatrix} \begin{Bmatrix} \overline{\boldsymbol{U}}_B \\ \overline{\boldsymbol{U}}_I \end{Bmatrix} = \omega^2 \begin{bmatrix} O & O \\ \boldsymbol{M}_{IB} & \boldsymbol{M}_{II} \end{bmatrix} \begin{Bmatrix} \overline{\boldsymbol{U}}_B \\ \overline{\boldsymbol{U}}_I \end{Bmatrix} \tag{15}$$

Thus, Eq. (15) will be used to calculate the natural frequencies of the free bending vibration of various AFGM Timoshenko beams with non-uniform cross-sections in the next section.

3 RESULTS AND DISCUSSIONS

In this section, the effects of material graded indices, height and width taper ratios, slenderness ratios, material compositions and restraint types on the free vibration characteristics of the AFGM Timoshenko beams are examined. Four types of AFGM beam constructed from Alumina and Stainless steel (A/S), Zirconia and Stainless steel (Z/S), Alumina and Aluminum (A/A), and Zirconia and Aluminum (Z/A), respectively, are considered. The material properties of the typical metals and ceramics are given in Table 2 (Shahba et al. (2011); Natarajon et al. (2011)). For simplicity, the Poisson's ratio is taken to be 0.3. It is assumed that the left side of the beam is ceramic-rich and the right side is metal-rich. The following frequency parameter $\boldsymbol{\lambda} = \omega L^2 \sqrt{\rho_{al} A_o / E_{al} I_o}$ is used to evaluate the dimensionless natural frequencies, in which E_{al} and ρ_{al} denote the Young's modulus and density of aluminum, respectively. The rotary inertial parameter r and slenderness ratio s are defined as I_o/A_oL^2 and $(1/r)^{0.5}$, respectively.

Table 2 Properties of materials.

material	E, GPa	ρ, Kg/m^3
Aluminum (Al)	70.0	2702
Stainless steel (SUS304)	201.04	8166
Alumina (Al_2O_3)	380.0	3800
Zirconia (ZrO_2)	200.0	5700

3.1 Model verification

To validate the accuracy of the proposed model, the free vibration of various exponential AFGM beams composed of zirconia and aluminum with L = 1m, b_o = 0.01m and h_o = 0.03m (Liu et al. (2016)) is studied. The A/Z AFGM beam is aluminum rich near x = 0 and zirconia rich near x = L, whereas the Z/A AFGM beam is vice versa. Because there is a lack of data of exponential AFGM Timoshenko beams in the published literature, the presented results are compared with those obtained by the Euler-Bernoulli beam theory. Table 3 present the first four dimensionless natural frequencies of uniform A/Z AFGM beams of α = 3 under various boundary conditions. The present results match well with those obtained by Huang and Li (2010), Liu et al. (2016) and Cao et al. (2018), especially the lower frequencies.

Table 4 gives the first four dimensionless natural frequencies of uniform pinned-pinned and clamped-clamped Z/A AFGM beams with various values of α. Likewise, the presented lower mode frequencies are in good agreement with those given by Huang and Li (2010) and Liu et al. (2016). The first four dimensionless natural frequencies of non-uniform clamped-free and clamped-pinned Z/A AFGM beams of α = -10 with various values of taper ratios are presented in Table 5. Good agreement is also observed between the present results and those by Liu et al. (2016). It is noted in Tables 3-5 that the discrepancy between the higher mode frequencies is greater than that of lower ones because the Euler-Bernoulli beam theory always overestimates the frequencies, especially for the higher modes. Hence, to provide more accurate results for exponential AFGM beams, the Timoshenko beam theory is also needed. In this study, only the bending vibration about the y-axis is considered. If the 3D finite element FGM beam is modeled according to the introduction of Murin et al. [2014, 2016], in addition to obtaining the same natural frequency of the bending mode about the y-axis as the proposed method, the natural frequencies of other bending modes around the z-axis, torsional modes and axial modes will also be determined.

3.2 Effect of taper ratio

Figures 3-6 present the effects of various values of C_h and C_b on the varying trend of the first four dimensionless frequencies for the CF and PP Z/A AFGM beams with r = 0.01 and α = -10. The variations of the first four natural frequencies with respect to the taper ratios C_h and C_b for the CP and CC Z/A AFGM beams are presented in Tables 6 and 7.

As can be seen, the increase in height and width taper ratios may decrease or increase the natural frequencies depending on the taper ratios and boundary conditions.

Table 3 Comparison of frequencies of uniform A/Z AFGM beams with different boundary conditions.

BC	source	λ_1	λ_2	λ_3	λ_4
CF	Present	2.8527	21.3863	62.9192	123.8613
	Huang and Li (2010)	2.8544	-	-	-
	Liu et al. (2016)	2.8545	21.4951	63.6755	126.6073
	Cao et al. (2018)	2.852	21.494	63.673	126.575
PP	Present	10.3513	41.7155	93.2389	164.0748
	Huang and Li (2010)	10.3669	-	-	-
	Liu et al. (2016)	10.3669	41.9691	94.5153	168.0682
	Cao et al. (2018)	10.368	41.973	94.510	167.997
CP	Present	15.6585	52.2805	108.5191	183.6220
	Huang and Li (2010)	15.7171	-	-	-
	Liu et al. (2016)	15.7169	52.8041	110.6243	189.4610
	Cao et al. (2018)	15.718	52.807	110.611	189.356
CC	Present	24.7797	66.1549	127.0355	206.2868
	Huang and Li (2010)	24.9375	-	-	-
	Liu et al. (2016)	24.9366	67.1081	130.2588	214.4078
	Cao et al. (2018)	24.942	67.113	130.236	214.258

Table 4 Comparison of frequencies of uniform PP and CC Z/A AFGM beams with different *α*.

BC	*α*	source	λ_1	λ_2	λ_3	λ_4
PP	-10	Present	9.9225	39.8335	89.3251	157.4965
		Huang and Li (2010)	9.9358	-	-	-
		Liu et al. (2016)	9.9366	40.07	90.5367	161.3146
	-3	Present	10.3513	41.7155	93.2389	164.0748
		Huang and Li (2010)	10.3669	-	-	-
		Liu et al. (2016)	10.3669	41.9691	94.5153	168.0682
	0	Present	10.8486	43.3957	96.7930	170.2173
		Huang and Li (2010)	10.8663	-	-	-
		Liu et al. (2016)	10.8664	43.6649	98.1296	174.3787
	3	Present	11.2250	44.5707	99.4306	174.8680
		Huang and Li (2010)	11.2443	-	-	-
		Liu et al. (2016)	11.2443	44.855	100.8244	179.1822
	10	Present	11.4367	45.3939	101.2149	177.9781
		Huang and Li (2010)	11.4532	-	-	-
		Liu et al. (2016)	11.4560	45.6887	102.6601	182.4345
CC	-10	Present	24.6463	65.2907	124.5252	201.2268
		Huang and Li (2010)	24.7949	-	-	-
		Liu et al. (2016)	24.8068	66.2401	127.6871	209.1345
	-3	Present	24.7797	66.1549	127.0355	206.2868
		Huang and Li (2010)	24.9375	-	-	-
		Liu et al. (2016)	24.9366	67.1081	130.2588	214.4078
	0	Present	24.2226	66.6214	129.5533	211.6095
		Huang and Li (2010)	24.3752	-	-	-
		Liu et al. (2016)	24.3756	67.5918	132.8706	220.0032
	3	Present	23.7942	66.7804	131.0912	215.1447
		Huang and Li (2010)	23.9456	-	-	-
		Liu et al. (2016)	23.9446	67.7638	134.4815	223.7508
	10	Present	23.9070	67.1197	131.9397	216.9219
		Huang and Li (2010)	24.0576	-	-	-
		Liu et al. (2016)	24.0660	68.1328	135.4215	225.7493

For CF beams shown in Figure 3, when C_h increases, the first frequency increases, while the other three frequencies show a downward trend. Basically, as the value of C_h is higher, the rate of change of frequency is more significant. As shown in Figure 4, with the increase in C_b, the first four frequencies rise. Similarly, as the value of C_b is larger, the rate of change of frequency is more obvious. For the first and second frequencies, the effect of C_b on the frequency is more significant than that of C_h, while for the third and fourth frequencies, the influence of C_h is greater. For PP beams in Figure 5, the first four frequencies are basically reduced with the increasing C_h, except that the fourth frequency of the beam with $C_b \leq 0.7$ increases slightly from $C_h = 0.1$ to 0.2. Its frequency is significantly affected by C_h, especially the first frequency. It can be seen from Figure 6 that as C_b increases, except for some cases, most of the frequencies of the PP beams decrease. The exception examples are as follows. The fourth frequency of the beam with $C_h = 0.1$ increases as C_b increases; for the beam with $C_h = 0.7$, the second and third frequencies first increase with C_b until $C_b = 0.8$ and then start to decrease, while the fourth frequency first decreases, then increases and then reduces; the second to fourth frequencies of the beam with $C_h = 0.9$ increase with the increasing C_b. Unlike CF beams, C_h has a more significant effect on the four frequencies of PP beams than C_b, but the effect of C_b is minor except for the first frequency.

Table 5 Comparison of frequencies of CF and CP Z/A AFGM beams with different C_b and C_h

BC	C_b/C_h	source	λ_1	λ_2	λ_3	λ_4
CF	0.2	Present	4.5077	23.2314	60.2770	113.9612
		Liu et al. (2016)	4.5112	23.3314	60.8734	116.0144
	0.4	Present	4.9642	22.0994	54.7752	102.1867
		Liu et al. (2016)	4.9675	22.1766	55.2115	103.6541
	0.6	Present	5.6549	20.9527	48.8786	89.3191
		Liu et al. (2016)	5.6563	21.0079	49.1851	90.3173
	0.8	Present	6.8815	20.0508	42.5236	74.7412
		Liu et al. (2016)	6.8715	20.0744	42.7624	75.5952
CP	0.2	Present	16.2118	48.8114	98.3631	164.2458
		Liu et al. (2016)	16.2634	49.2161	99.916	168.486
	0.4	Present	15.0674	43.8500	87.5967	145.8939
		Liu et al. (2016)	15.1061	44.1433	88.7009	148.8877
	0.6	Present	13.7489	38.4115	75.7276	125.5016
		Liu et al. (2016)	13.7727	38.6134	76.4763	127.5011
	0.8	Present	12.1312	32.1014	61.8686	101.4631
		Liu et al. (2016)	12.1299	32.2583	62.5395	103.3128

As for the CP beams in Table 6, when C_h increases, except that the fourth frequency increases slightly from $C_h = 0.1$ to 0.2, all other frequencies decrease accordingly. With the increasing C_b, basically the first frequency increases. Except for beams with $C_h = 0.1$ and 0.2, their first frequency decreases slightly when C_b increases from 0.8 to 0.9. For beams with $C_h \leq 0.6$, the second to fourth frequencies first increase and then decrease with the increase of C_b, and for beams with $C_h \geqq 0.7$, they increase accordingly. Like the PP beams, the influence of C_h on the frequency is significant, while the effect of C_b is minimal. For CC beams in Table 7, when C_h enlarges, all frequencies decrease. As C_b increases, all frequencies first increase and then decrease for beams with $C_h \leq 0.8$. In addition, when the beam has a higher C_h value, the C_b value at which the frequency changes from rising to falling is greater. When the beam has a taper of $C_h = 0.9$, all frequencies rise with the increasing C_b. Like PP and CP beams, C_h has a significant impact on the frequency, while C_b has a slight impact.

As discussed above, the natural frequencies for the beams with the same width ratio C_b reduce with the increasing height taper ratio C_h except for the first frequencies of CF beams and fourth frequencies of PP and CP beams. As for the beams with the same height taper ratio C_h, the first four frequencies of CF beams increase with the increasing width taper ratio C_b but those of PP, CP and CC beams vary differently with C_b depending on the value of C_h. It is important to note that the height taper ratio has a more profound impact on the natural frequencies of all beams than width taper ratio while it shows an opposite trend for the first and second frequencies of CF beams.

3.3 Effect of material distribution

Table 8 gives the effects of material graded index α on the first four frequencies of Z/A AFGM beams of $r = 0.01$ and $C_b/C_h = 0.3/0.5$ under various boundary conditions. As can be seen, the first and second frequencies of the CF beam reduce as the value of $|\alpha|$ approaches to zero, but its third and fourth frequencies enlarge with the increasing α. For the PP beam, all the first four frequencies increase with the increase in α. For the CP and CC beams, the first and second modes varies irregularly with α, but the third and fourth modes increase as α increases.

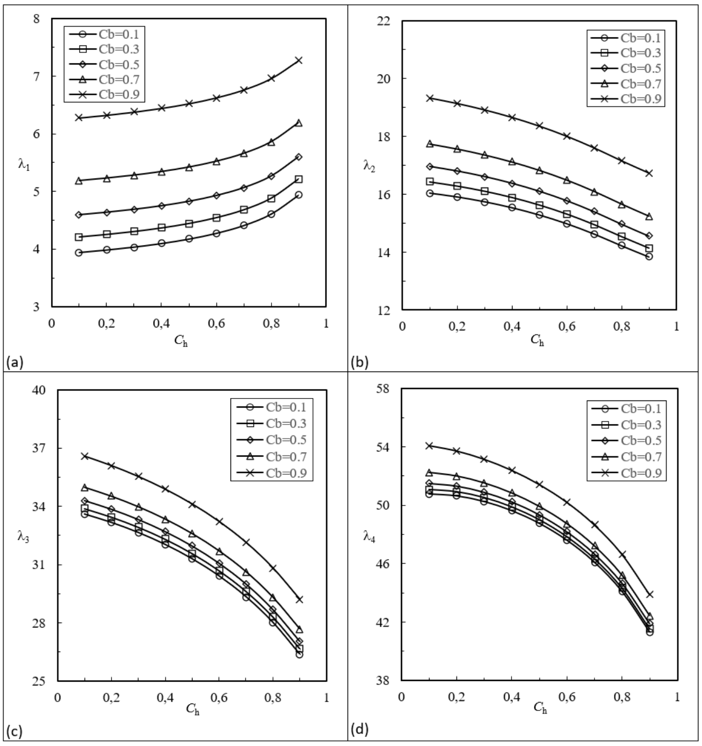

Figure 3: Effect of C_h on dimensionless natural frequencies for clamped-free Z/A AFGM beams of r = 0.01 and α = -10 with various values of C_b. (a) First mode (b) Second mode (c) Third mode (d) Fourth mode

3.4 Effect of slenderness ratio

Table 9 shows the effects of the slenderness ratio *s* on the first four frequencies of Z/A AFGM beams of α = 3 and C_b/C_h = 0.5/0.5 under different boundary conditions. As expected, all frequencies decrease with the increasing *s*. The influence is becoming more significant for higher mode frequencies and restraint.

3.5 Effect of material composition

Tables 10-13 give the variations of the natural frequencies against different material constituents of uniform and non-uniform AFGM beams of *r* = 0.01 with CF, PP, CP and CC boundary conditions, respectively. As far as CF beams are concerned, except for some exceptions, basically A/A beam has the largest frequency, followed by A/S, Z/A and Z/S beams. However, when α = 0 and -3, the order of the first mode frequency is A/A > Z/A > A/S > Z/S, and Z/A is larger than A/S. Similarly, the first four frequencies of the Z/A beam are larger than those of the A/S beam as α = -10. Furthermore, it can be seen from Table 10 that different material compositions have a significant effect on the frequency of the CF beam, and the influence is different under different values of α.

For PP beams, in most cases, the order of frequencies of beams composed of different materials is A/A, A/S, Z/A and Z/S beams from high to low. The exceptions are as follows. When α = -10, the first frequency of uniform Z/A beam is larger than that of A/S beam; when α = -3, 0 and 3, the first frequency of non-uniform Z/S beam is greater than that of Z/A beam. For uniform beam with α = 10, the order of the first three frequencies from high to low is the A/A, A/S, Z/S and Z/A beams. For nonuniform beam with α = 10, the order of the first frequency is the A/S, A/A, Z/S and Z/A beams, and that of second to fourth frequencies is A/A, A/S, Z/S and Z/A beams. In addition, it can be found from Table 11 that the difference between the frequencies of A/A and A/S beams is small, especially when α = 10, the discrepancy is even smaller. The same phenomenon also occurs between Z/A and Z/S beams. When α = -10, the difference of frequencies among the four beams A/A, A/S, Z/A and Z/S is very small.

Like the CF and PP beams, the order of frequencies for the four types of CP beams is A/A, A/S, Z/A and Z/S beams except for some typical cases. For example, the order of frequencies becomes A/A, Z/A, A/S and Z/S for all four frequencies of beams with α = -10, and for the first frequency of nonuniform beams with α = -3. In addition, as α = 10, the first three frequencies of the uniform Z/S beam and the first four frequencies of the nonuniform Z/S beam are larger than those of the corresponding Z/A beam. As can be seen in Table 12, when α = 10, the difference between the frequencies of A/A and A/S beams is small except for the third and fourth frequencies of the beams with uniform cross-section. The same phenomenon also occurs between Z/A and Z/S beams.

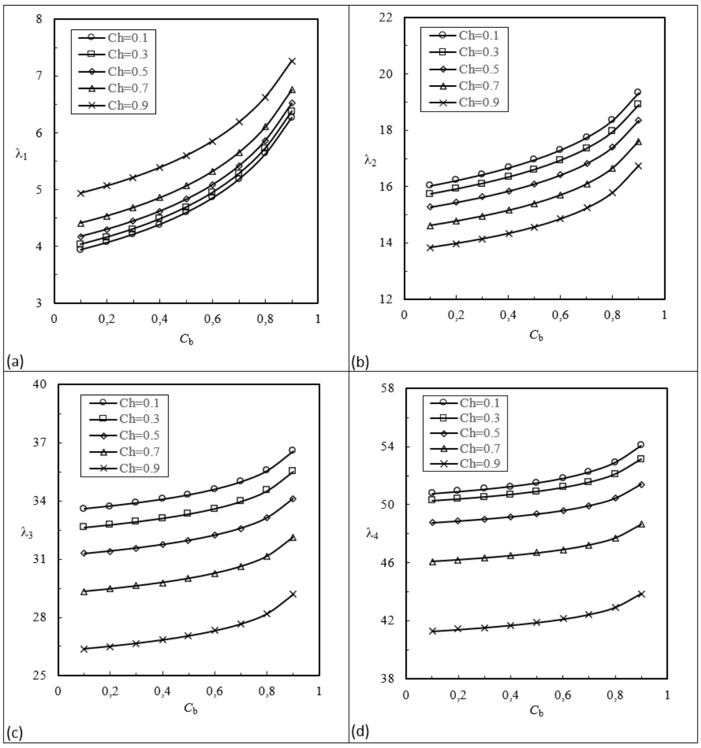

Figure 4: Effect of C_b on dimensionless natural frequencies for clamped-free Z/A AFGM beams of r = 0.01 and α = -10 with various values of C_h. (a) First mode (b) Second mode (c) Third mode (d) Fourth mode.

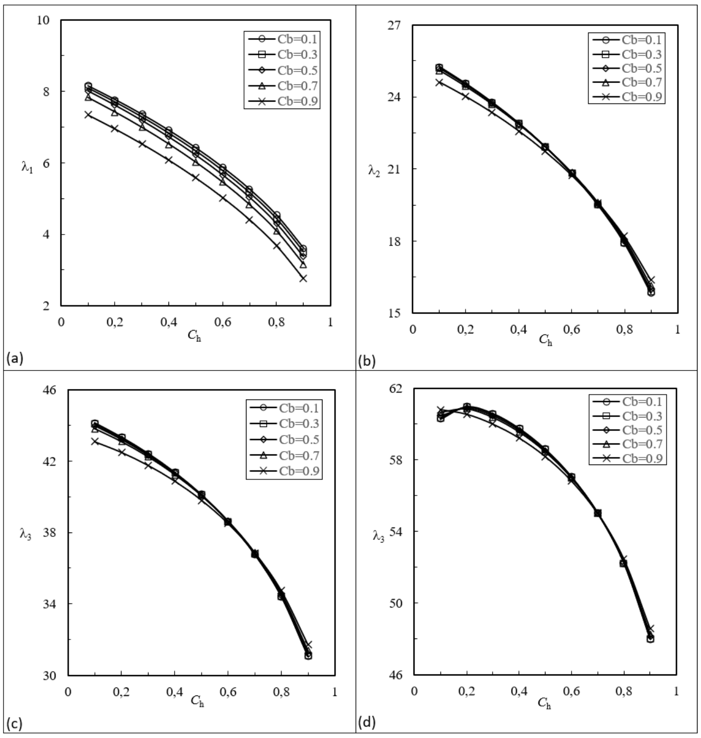

Figure 5: Effect of C_h on dimensionless natural frequencies for pinned-pinned Z/A AFGM beams of r = 0.01 and α = -10 with various values of C_b. (a) First mode (b) Second mode (c) Third mode (d) Fourth mode.

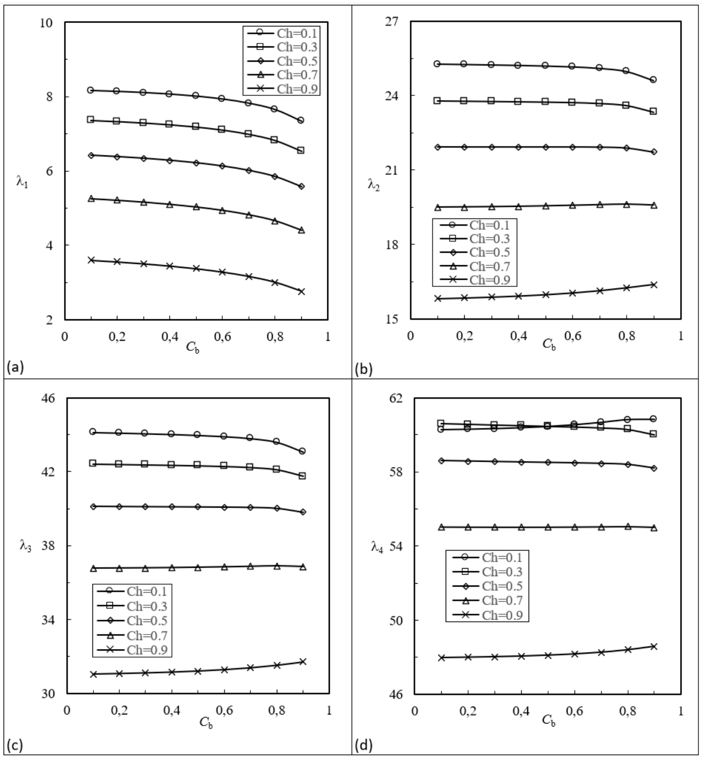

Figure 6: Effect of C_b on dimensionless natural frequencies for pinned-pinned Z/A AFGM beams of r = 0.01 and α = -10 with various values of C_h. (a) First mode (b) Second mode (c) Third mode (d) Fourth mode.

For CC beams, basically A/A beam has the largest frequency, followed by A/S, Z/A and Z/S beams except for some exceptions. Like CF and CP beams, the order of frequencies is A/A, Z/A, A/S and Z/S for the beams with α = -10; however, the difference between the frequencies of Z/A and A/S beams is slight. When α = 3, the first and second frequencies of uniform Z/A beam and the first frequency of non-uniform Z/A beam are larger than those of the corresponding Z/A beam. When α = 10, the order of frequencies is A/S, A/A, Z/S and Z/A for the first and second frequencies, and is A/A, A/S, Z/S and Z/A for the third and fourth frequencies.

Table 6 Effects of height and width taper ratios on first four dimensionless natural frequencies of clamped-pinned Z/A AFGM beams with r = 0.01 and α = -10.

C_b	mode	C_h=0.1	C_h =0.2	C_h =0.3	C_h =0.4	C_h =0.5	C_h =0.6	C_h =0.7	C_h =0.8	C_h =0.9
0.1	λ_1	12.2065	11.9714	11.7033	11.3953	11.0379	10.6166	10.1079	9.4669	8.5802
	λ_2	28.9014	28.3459	27.7170	26.9975	26.1633	25.1783	23.9841	22.4723	20.3792
	λ_3	47.0944	46.4158	45.6239	44.6907	43.5757	42.2166	40.5109	38.2658	35.0143
	λ_4	64.0744	64.8251	64.0596	63.0676	61.8341	60.2800	58.2625	55.5058	51.3275
0.2	λ_1	12.3043	12.0668	11.7966	11.4867	11.1278	10.7054	10.1961	9.5555	8.6714
	λ_2	28.9592	28.4085	27.7845	27.0702	26.2414	25.2622	24.0742	22.5691	20.4841
	λ_3	47.1392	46.4636	45.6757	44.7474	43.6379	42.2852	40.5868	38.3504	35.1099
	λ_4	64.1128	64.8491	64.0947	63.1093	61.8819	60.3342	58.3243	55.5766	51.4102
0.3	λ_1	12.4078	12.1681	11.8958	11.5843	11.2240	10.8008	10.2915	9.6521	8.7720
	λ_2	29.0171	28.4720	27.8539	27.1457	26.3234	25.3510	24.1705	22.6738	20.5989
	λ_3	47.1837	46.5119	45.7287	44.8059	43.7030	42.3577	40.6679	38.4418	35.2143
	λ_4	64.1523	64.8693	64.1290	63.1515	61.9313	60.3913	58.3901	55.6530	51.5006
0.4	λ_1	12.5170	12.2751	12.0011	11.6882	11.3271	10.9036	10.3950	9.7578	8.8836
	λ_2	29.0733	28.5352	27.9243	27.2236	26.4092	25.4453	24.2740	22.7876	20.7258
	λ_3	47.2267	46.5595	45.7820	44.8660	43.7708	42.4344	40.7550	38.5412	35.3298
	λ_4	64.1908	64.8830	64.1610	63.1937	61.9822	60.4514	58.4607	55.7364	51.6010
0.5	λ_1	12.6306	12.3870	12.1117	11.7981	11.4368	11.0139	10.5071	9.8738	9.0082
	λ_2	29.1245	28.5955	27.9938	27.3026	26.4982	25.5450	24.3853	22.9123	20.8676
	λ_3	47.2653	46.6043	45.8342	44.9267	43.8411	42.5157	40.8491	38.6507	35.4596
	λ_4	64.2232	64.8851	64.1880	63.2341	62.0340	60.5148	58.5372	55.8286	51.7144

Table 6 Continued...

C_b	mode	C_h=0.1	C_h =0.2	C_h =0.3	C_h =0.4	C_h =0.5	C_h =0.6	C_h =0.7	C_h =0.8	C_h =0.9
0.6	λ_1	12.7457	12.5012	12.2256	11.9122	11.5519	11.1311	10.6279	10.0010	9.1482
	λ_2	29.1636	28.6469	28.0577	27.3793	26.5882	25.6490	24.5049	23.0498	21.0285
	λ_3	47.2925	46.6407	45.8809	44.9848	43.9120	42.6010	40.9510	38.7727	35.6084
	λ_4	64.2382	64.8651	64.2036	63.2688	62.0843	60.5806	58.6201	55.9322	51.8459
0.7	λ_1	12.8543	12.6106	12.3364	12.0252	11.6682	11.2521	10.7557	10.1393	9.3059
	λ_2	29.1735	28.6751	28.1041	27.4442	26.6722	25.7532	24.6310	23.2014	21.2140
	λ_3	47.2908	46.6544	45.9106	45.0316	43.9773	42.6869	41.0603	38.9101	35.7837
	λ_4	64.2101	64.7991	64.1918	63.2871	62.1262	60.6452	58.7092	56.0504	52.0033
0.8	λ_1	12.9339	12.6947	12.4260	12.1214	11.7723	11.3660	10.8823	10.2841	9.4819
	λ_2	29.1069	28.6391	28.0984	27.4688	26.7277	25.8411	24.7538	23.3643	21.4308
	λ_3	47.2069	46.6006	45.8861	45.0370	44.0140	42.7574	41.1686	39.0631	35.9970
	λ_4	64.0728	64.6223	64.1040	63.2531	62.1338	60.6916	58.7964	56.1844	52.2003
0.9	λ_1	12.9026	12.6786	12.4264	12.1400	11.8112	11.4281	10.9720	10.4094	9.6633
	λ_2	28.7869	28.3819	27.9032	27.3356	26.6572	25.8353	24.8168	23.5049	21.6736
	λ_3	46.8249	46.2894	45.6429	44.8614	43.9078	42.7242	41.2149	39.2006	36.2550
	λ_4	63.6041	64.0978	63.7358	63.0009	61.9761	60.6216	58.8161	56.3048	52.4515

Table 7 Effects of height and width taper ratios on first four dimensionless natural frequencies of clamped-clamped Z/A AFGM beams with r = 0.01 and α = -10.

C_b	mode	C_h=0.1	C_h =0.2	C_h =0.3	C_h =0.4	C_h =0.5	C_h =0.6	C_h =0.7	C_h =0.8	C_h =0.9
0.1	λ_1	14.8824	14.5528	14.1730	13.7316	13.2127	12.5931	11.8356	10.8724	9.5396
	λ_2	30.3509	29.9441	29.4565	28.8636	28.1301	27.2031	25.9969	24.3530	21.8923
	λ_3	47.8869	47.3767	46.7752	46.0503	45.1537	44.0076	42.4793	40.3139	36.8848
	λ_4	65.0555	64.8950	64.4427	63.7667	62.8556	61.6376	59.9575	57.4856	53.3667
0.2	λ_1	14.8865	14.5635	14.1909	13.7573	13.2469	12.6365	11.8891	10.9374	9.6183
	λ_2	30.3541	29.9536	29.4731	28.8882	28.1640	27.2477	26.0540	24.4249	21.9824
	λ_3	47.8936	47.3872	46.7901	46.0708	45.1809	44.0434	42.5261	40.3748	36.9648
	λ_4	65.0694	64.9099	64.4593	63.7862	62.8792	61.6672	59.9955	57.5357	53.4347
0.3	λ_1	14.8818	14.5665	14.2023	13.7778	13.2774	12.6780	11.9429	11.0051	9.7031
	λ_2	30.3469	29.9537	29.4814	28.9060	28.1927	27.2891	26.1102	24.4988	22.0786
	λ_3	47.8927	47.3904	46.7984	46.0854	45.2034	44.0759	42.5714	40.4369	37.0499
	λ_4	65.0784	64.9197	64.4711	63.8011	62.8990	61.6939	60.0321	57.5865	53.5070
0.4	λ_1	14.8641	14.5578	14.2036	13.7900	13.3016	12.7155	11.9954	11.0749	9.7946
	λ_2	30.3244	29.9398	29.4773	28.9132	28.2129	27.3245	26.1636	24.5740	22.1817
	λ_3	47.8801	47.3827	46.7966	46.0909	45.2183	44.1027	42.6136	40.4995	37.1409
	λ_4	65.0795	64.9217	64.4752	63.8091	62.9125	61.7156	60.0656	57.6373	53.5841
0.5	λ_1	14.8265	14.5313	14.1890	13.7888	13.3150	12.7454	12.0439	11.1453	9.8931
	λ_2	30.2784	29.9041	29.4536	28.9032	28.2189	27.3494	26.2109	24.6487	22.2920
	λ_3	47.8494	47.3576	46.7785	46.0817	45.2204	44.1194	42.6494	40.5607	37.2382
	λ_4	65.0679	64.9108	64.4669	63.8052	62.9155	61.7286	60.0932	57.6865	53.6667
0.6	λ_1	14.7576	14.4758	14.1485	13.7648	13.3096	13.3096	12.0833	11.2132	9.9980
	λ_2	30.1942	29.8330	29.3974	28.8644	28.2004	28.2004	26.2452	24.7187	22.4095
	λ_3	47.7884	47.3034	46.7330	46.0471	45.2000	45.2000	42.6721	40.6166	37.3419
	λ_4	65.0337	64.8774	64.4368	63.7807	62.8996	62.8996	60.1087	57.7302	53.7548
0.7	λ_1	14.6352	14.3707	14.0626	13.7003	13.2693	12.7479	12.1024	11.2708	10.1067
	λ_2	30.0432	29.6990	29.2831	28.7730	28.1360	27.3226	26.2520	24.7744	22.5317
	λ_3	47.6721	47.1959	46.6366	45.9650	45.1366	44.0790	42.6670	40.6573	37.4499
	λ_4	64.9561	64.8007	64.3646	63.7161	62.8463	61.6891	60.0982	57.7589	53.8466
0.8	λ_1	14.4105	14.1696	13.8878	13.5552	13.1577	12.6750	12.0748	11.2986	10.2095
	λ_2	29.7586	29.4383	29.0501	28.5725	27.9742	27.2073	26.1937	24.7886	22.6471
	λ_3	47.4394	46.9751	46.4310	45.7796	44.9781	43.9567	42.5941	40.6538	37.5510
	λ_4	64.7807	64.6270	64.1978	63.5603	62.7071	61.5750	60.0227	57.7437	53.9310
0.9	λ_1	13.9380	13.9380	13.4932	13.2073	12.8633	12.4425	11.9156	11.2302	10.2660
	λ_2	29.1297	29.1297	28.5043	28.0799	27.5454	26.8564	25.9397	24.6601	22.6983
	λ_3	46.8820	46.8820	45.9157	45.2967	44.5396	43.5798	42.3039	40.4884	37.5807
	λ_4	64.3146	64.3146	63.7456	63.1264	62.3008	61.2118	59.7281	57.5607	53.9405

Table 8 Effects of material graded index on frequencies of various Z/A AFGM beams.

BC	α	λ1	λ2	λ3	λ4	BC	λ1	λ2	λ3	λ4
	-10	4.4449	15.6333	31.5733	49.0082		11.2240	26.3234	43.7030	61.9313
	-6	4.7360	16.0390	31.9440	49.4211		11.5645	26.6980	44.0827	62.4317
	-3	5.1041	16.4705	32.4667	50.2388		11.7772	27.0205	44.6817	63.4477
	-1	5.3236	16.8374	33.1053	51.2962		11.7684	27.2512	45.3244	64.5875
CF	0	5.3711	17.0255	33.4843	51.9289	CP	11.7147	27.3401	45.6578	65.1886
	1	5.3679	17.1903	33.8568	52.5492		11.6489	27.3992	45.9494	65.7212
	3	5.2635	17.3947	34.4629	53.5557		11.1095	26.5020	44.9540	64.8457
	6	5.0704	17.4458	34.9346	54.3723		11.4976	27.5056	46.5920	66.8996
	10	4.9061	17.3522	35.0900	54.7309		11.5288	27.5944	46.7064	67.0535
	-10	6.3385	21.9220	40.1004	58.5499		13.2774	28.1927	45.2034	62.8990
	-6	6.3464	22.2698	40.8144	59.9231		13.5840	28.5568	45.5729	63.3914
	-3	6.4251	22.9635	42.0355	61.8303		13.6585	28.8164	46.1405	64.3744
	-1	6.5629	23.6002	43.1299	63.4739		13.4927	28.9129	46.6805	65.4279
PP	0	6.6543	23.8775	43.6413	64.2556	CC	13.3628	28.9104	46.9297	65.9575
	1	6.7500	24.0898	44.0632	64.9168		13.2346	28.8790	47.1278	66.4091
	3	6.9224	24.3319	44.5923	65.7838		13.0560	28.7960	47.3573	66.9936
	6	7.0951	24.4701	44.8820	66.2848		12.9954	28.7607	47.4672	67.3065
	10	7.2110	24.5691	45.0015	66.4534		13.0706	28.8478	47.5311	67.3932

4 CONCLUSION

The eigenvalue problem for the free vibration of non-uniform AFGM Timoshenko beams with various boundary conditions is established based on the Chebyshev collocation method. The axially graded material properties of the beam are assumed to vary exponentially. Four types of AFGM Timoshenko beams constructed from two metals and two ceramics are examined to demonstrate the effect of material compositions on the vibration behavior. Based on the results discussed previously, some major conclusions are highlighted as follows.

1. Depending on the values of taper ratios and boundary conditions, the natural frequencies of AFGM beams may decrease or increase with the increasing height and width taper ratios. The height taper ratio has a more considerable effect on the natural frequencies than the width taper ratio except for the fundamental frequencies of clamped-free beams.
2. The variation of natural frequencies against the values of material graded index varies differently depending on the restraint types of the AFGM beams.
3. The natural frequencies of AFGM beams always reduce as the slenderness ratio increases.
4. Except for certain cases, basically the AFGM beam constructed from Alumina/Aluminum has the highest frequency, followed by the beams made from Alumina/Stainless steel, Zirconia/Aluminum and Zirconia/Stainless steel.

Table 9 Effects of slenderness ratios on frequencies of various Z/A AFGM beams (C_b = C_h =0.5,α = 3).

BC	s	λ1	λ2	λ3	λ4	BC	λ1	λ2	λ3	λ4
	10	5.7011	17.9226	34.9082	53.9387		11.731	27.6358	46.4857	66.5543
	15	5.9881	20.6172	42.9089	69.3777		13.1636	33.6959	59.4700	88.0143
	20	6.1005	21.9200	47.6079	79.6896		13.8128	37.0702	67.9055	103.3178
CF	25	6.1551	22.6208	50.4574	86.6044	CP	14.1499	39.0461	73.4191	114.1922
	40	6.2160	23.4693	54.3028	97.0140		14.5468	41.6252	81.4737	131.7932
	50	6.2304	23.6805	55.341	100.0918		14.6436	42.3037	83.7941	137.3496
	100	6.2497	23.9721	56.8369	104.7746		14.776	43.2677	87.2673	146.1852
	10	6.7599	24.3585	44.6278	65.8059		13.1016	28.8576	47.4069	67.0408
	15	7.2278	28.0742	54.9724	84.9724		15.2398	36.3062	61.9987	90.1096
	20	7.4158	29.9270	61.0578	97.6454		16.2932	40.7546	72.0013	107.2412
PP	25	7.5079	30.9446	64.7891	106.1477	CC	16.865	43.4808	78.8019	119.8109
	40	7.6118	32.2006	69.9106	119.0740		17.5624	47.1965	89.1769	140.9745
	50	7.6364	32.5176	71.3156	122.9491		17.7367	48.2071	92.2766	147.8983
	100	7.6696	32.9587	73.3607	128.9128		17.978	49.669	97.0215	159.1885

Table 10 Effects of material constituents on frequencies of CF AFGM beams with various α.

α	material	C_b/C_h = 0/0				C_b/C_h = 0.5/0.5			
		λ_1	λ_2	λ_3	λ_4	λ_1	λ_2	λ_3	λ_4
-10	A/A	4.2407	17.3452	36.7106	54.1636	5.2641	17.4238	34.7033	53.6431
	A/S	**3.4635**	**15.1064**	**32.9028**	**49.6085**	**4.4771**	**15.2588**	**30.9632**	**48.5644**
	Z/A	**3.7918**	**15.9645**	**33.8195**	**50.5106**	**4.8266**	**16.1044**	**31.9656**	**49.3529**
	Z/S	3.1448	14.1531	30.992	47.1774	4.1551	14.3498	29.1613	45.8307
-3	A/A	5.6059	21.3784	43.4724	62.8835	6.9669	21.1439	41.0803	63.0698
	A/S	**3.875**	17.0318	37.0995	55.06	**5.0078**	17.0696	34.8605	54.641
	Z/A	**4.3605**	16.9558	34.7398	51.7567	**5.5327**	16.9568	32.884	50.6078
	Z/S	3.1704	14.5222	32.0209	48.585	4.1934	14.7138	30.096	47.3152
0	A/A	6.4529	25.1721	51.2134	75.0721	8.2321	24.871	48.0182	73.7759
	A/S	**4.3246**	19.8436	43.1684	63.4144	**5.6524**	19.8083	40.4538	63.2824
	Z/A	**4.5345**	17.5155	36.0084	53.974	**5.8175**	17.532	33.9186	52.3087
	Z/S	3.2427	15.1066	33.2936	50.4004	4.2971	15.2923	31.2935	49.1456
3	A/A	6.7457	27.7939	57.7151	86.4316	8.7695	27.7849	53.9775	83.2066
	A/S	4.8343	23.2556	50.4095	74.3115	6.4048	23.2375	47.2026	73.7243
	Z/A	4.3993	17.7526	37.139	56.0609	5.7011	17.9226	34.9082	53.9387
	Z/S	3.3613	15.7716	34.5996	52.3815	4.4635	15.9493	32.5453	51.0777
10	A/A	6.6132	28.8966	61.9925	93.9433	8.684	29.2976	58.2359	90.3294
	A/S	5.4852	26.3022	57.3188	86.2491	7.336	26.4074	53.7874	84.2747
	Z/A	4.0727	17.567	37.7038	57.0976	5.3226	17.8817	35.5365	55.1159
	Z/S	3.5407	16.3291	35.7071	54.2395	4.7053	16.5007	33.5938	52.7644

Table 11 Effects of material constituents on frequencies of PP AFGM beams with various α.

α	material	C_b/C_h = 0/0				C_b/C_h = 0.5/0.5			
		λ_1	λ_2	λ_3	λ_4	λ_1	λ_2	λ_3	λ_4
-10	A/A	8.8664	27.4786	47.8341	59.8793	6.3997	23.1266	42.6276	62.7588
	A/S	**8.4198**	25.9397	45.3942	**57.2846**	6.2201	21.9996	40.5579	59.919
	Z/A	**8.5267**	25.9028	44.8624	**57.7733**	6.2179	21.9227	40.0867	58.5017
	Z/S	8.2201	24.958	43.5423	55.9143	6.1323	21.3072	39.0531	57.6134
-3	A/A	10.6897	33.0346	57.5276	67.5994	10.4433	37.1765	67.9696	100.2559
	A/S	9.4849	29.2753	51.1403	61.2772	7.0276	25.0824	46.3365	68.5972
	Z/A	8.8228	26.9453	46.8939	60.1156	**6.2749**	22.9964	42.0643	61.831
	Z/S	8.464	25.7594	44.9141	57.2414	**6.3219**	21.9406	40.2334	59.3569
0	A/A	12.8424	38.7404	67.2071	80.6633	8.9885	33.2007	60.7103	89.4888
	A/S	11.2784	34.1054	59.3382	68.2911	8.2376	28.8449	53.0091	78.319
	Z/A	9.1309	27.8616	48.5051	62.5079	**6.4899**	23.9202	43.6864	64.2787
	Z/S	8.8599	26.8129	46.6825	59.1575	**6.6225**	22.8072	41.7885	61.6342
3	A/A	14.6211	43.0527	74.4581	94.5451	10.4433	37.1765	67.9696	100.2559
	A/S	13.6134	39.9668	69.154	78.7618	10.0147	33.8532	61.9486	91.4141
	Z/A	9.3801	28.3156	49.3606	64.2676	**6.7599**	24.3585	44.6278	65.8059
	Z/S	9.3202	27.9761	48.6421	61.5743	**6.9666**	23.8056	43.5472	64.1858
10	A/A	15.881	46.5378	79.7792	104.2693	**11.6719**	40.062	73.0138	107.6481
	A/S	15.847	46.3248	79.618	94.9312	**11.7854**	39.4761	71.4935	105.0894
	Z/A	**9.5922**	**28.6606**	**49.7154**	64.9673	**7.0678**	**24.5677**	**45.0052**	**66.451**
	Z/S	**9.6864**	**29.0776**	**50.4829**	64.2444	**7.2314**	**24.8136**	**45.251**	**66.5883**

Table 12 Effects of material constituents on frequencies of CP AFGM beams with various α.

α	material	C_b/C_h = 0/0				C_b/C_h = 0.5/0.5			
		λ_1	λ_2	λ_3	λ_4	λ_1	λ_2	λ_3	λ_4
-10	A/A	13.4086	31.9141	51.7972	60.6589	12.4419	28.7821	47.7042	67.473
	A/S	**11.5854**	**28.3555**	**46.8734**	**58.3731**	**10.7277**	**25.4807**	**42.969**	**61.5306**
	Z/A	**12.319**	**29.3431**	**47.6356**	**59.8765**	**11.4368**	**26.4982**	**43.8411**	**62.034**
	Z/S	10.8284	26.6431	44.2193	57.8264	10.0172	23.9578	40.4861	58.1459
-3	A/A	16.1067	37.4243	60.5469	67.922	14.9729	34.0094	55.9835	79.1177
	A/S	12.943	31.9443	52.7346	61.8067	**11.9371**	28.6847	48.4077	69.2369
	Z/A	12.8996	29.9434	48.5997	61.7129	**12.009**	27.2196	44.8408	63.5648
	Z/S	11.1031	27.5406	45.6941	58.725	10.2562	24.7268	41.8294	60.0317
0	A/A	18.3095	42.5087	69.604	80.8435	16.8835	38.8848	64.4856	91.6243
	A/S	15.0498	37.0281	61.0717	68.6256	13.792	33.2664	56.0399	80.0905
	Z/A	12.8934	30.2294	49.7045	64.17	11.9269	27.5404	45.8167	65.3032
	Z/S	11.6054	28.7343	47.5403	60.4789	10.7154	25.7909	43.5199	62.3875
3	A/A	19.9082	46.3528	76.5448	94.7805	18.2321	42.5569	71.2708	101.7936
	A/S	17.8761	43.2093	71.0487	78.9536	16.3508	38.8764	65.1843	93.1016
	Z/A	12.7625	30.3402	50.4258	65.8577	11.731	27.6358	46.4857	66.5543
	Z/S	12.2289	30.0166	49.5182	62.9734	11.3017	26.96	45.3385	64.9468
10	A/A	21.0633	49.7242	81.7484	104.7704	19.3448	45.3349	76.1384	108.9015
	A/S	20.838	49.7007	81.3255	95.3596	19.2254	44.7513	74.5742	106.4673
	Z/A	**12.7318**	**30.6158**	**50.776**	66.3049	**11.7118**	**27.7456**	**46.8167**	**67.1274**
	Z/S	**12.772**	**31.1434**	**51.3116**	66.2673	**11.8284**	**28.0172**	**47.0089**	**67.3071**

Table 13 Effects of material constituents on frequencies of CC AFGM beams with various α.

α	material	C_b/C_h = 0/0				C_b/C_h = 0.5/0.5			
		λ_1	λ_2	λ_3	λ_4	λ_1	λ_2	λ_3	λ_4
-10	A/A	16.3928	33.2057	52.3728	68.545	14.4628	30.5826	49.0851	68.2845
	A/S	**14.3816**	**29.6958**	**47.5981**	**63.5634**	**12.5403**	**27.1999**	**44.3711**	**62.391**
	Z/A	**15.1658**	**30.689**	**48.3179**	**64.7098**	**13.315**	**28.2189**	**45.2204**	**62.9155**
	Z/S	13.5305	28.0146	45.0219	60.8917	11.7341	25.6217	41.8916	59.0497
-3	A/A	18.8337	38.4425	60.892	80.7591	17.0061	35.8171	57.2714	79.7594
	A/S	15.9508	33.1948	53.3487	70.7978	13.9362	30.7379	50.3999	70.9856
	Z/A	15.3785	31.1742	49.2428	66.314	13.7252	28.8722	46.1803	64.4084
	Z/S	13.9302	28.9106	46.472	62.7747	12.0527	26.4381	43.2468	60.921
0	A/A	20.76	43.0964	69.619	94.8946	18.7636	40.4637	65.5041	92.0081
	A/S	18.4012	38.1384	61.4322	82.4457	16.0711	35.2132	57.4092	80.7298
	Z/A	15.0204	31.1424	50.0911	68.105	13.4244	28.9794	46.9808	66.0012
	Z/S	14.6114	30.1476	48.3098	65.3853	12.6283	27.5771	44.9712	63.2807
3	A/A	22.3598	46.735	76.5918	105.7572	20.0146	43.9052	72.0118	101.9661
	A/S	21.7512	44.291	71.1405	97.0267	18.9675	40.9782	66.5163	93.5989
	Z/A	**14.7603**	**31.0117**	50.5738	69.1699	**13.1016**	28.8576	47.4069	67.0408
	Z/S	**15.4105**	**31.538**	50.3355	68.3108	**13.3287**	28.8536	46.8658	65.8777
10	A/A	**24.0832**	**50.2262**	81.8225	112.7892	**21.2313**	**46.6646**	76.7595	108.9785
	A/S	**25.3428**	**51.3118**	81.5111	111.6912	**22.084**	**47.25**	76.1682	107.0005
	Z/A	**14.9451**	**31.2678**	**50.8351**	**69.5317**	**13.1039**	**28.8801**	**47.5586**	**67.427**
	Z/S	**16.0227**	**32.8202**	**52.2987**	**70.9749**	**13.8957**	**30.026**	**48.6867**	**68.363**

Acknowledgement

This work was supported by the Ministry of Science and Technology, Taiwan, R.O.C. [grant no. MOST-106-2221-E-034-012].

Author Contributions: Conceptualization, WR Chen; Methodology, WR Chen; Investigation, WR Chen; Software, WR Chen; Writing - original draft, WR Chen; Writing - review & editing, WR Chen; Funding acquisition, WR Chen.

Editor: Pablo Andrés Muñoz Rojas.

References

Boyd, J.P., (2000). Chebyshev and Fourier Spectral Methods, Second Edition, DOVER Publications, Inc. (New York).

Calim, F.F. (2016). Transient analysis of axially functionally graded Timoshenko beams with variable cross-section, Compos Part B: Eng 98:472-83.

Cao, D., Gao, Y., Yao, M., Zhang, W. (2018). Free vibration of axially functionally graded beams using the asymptotic development method, Eng Struct 173:442-48.

Chen W.R., Chang H. (2017). Closed-form solutions for free vibration frequencies of functionally graded Euler-Bernoulli beams, M Compos Mat 53:79-98.

Chen W.R., Chang H. (2018). Vibration analysis of functionally graded Timoshenko beams, Int J Struct Sta. Dyn 18:1850007.

Chen W.R. (2020). Vibration analysis of axially functionally graded tapered Euler-Bernoulli beams based on Chebyshev collocation method, Int. J. Acoustics Vib. 25:436-44.

Ding, J., Chu, L., Xin, L., Dui, G. (2018). Nonlinear vibration analysis of functionally graded beams considering the influences of the rotary inertia of the cross section and neutral surface position, Mech Based Des Struct Mach 46:225-37.

Esen, I. (2019). Dynamic response of a functionally graded Timoshenko beam on two-parameter elastic foundations due to a variable velocity moving mass, Int J Mech Sci 153-154:21-35.

Gottlieb, D. and Orszag, S.A., (1977). Numerical Analysis of Spectral Methods: Theory and Applications, SIAM (Philadelphia).

Hein, H., Feklistova, L. (2011). Free vibrations of non-uniform and axially functionally graded beams using Haar wavelets, Eng Struct 33:3696–701.

Huang, Y., Li, X.F. (2010). A new approach for free vibration of axially functionally graded beams with non-uniform cross-section, J Sound Vib 329:2291-303.

Huang, Y., Yang, L.E., Luo, Q.Z. (2013). Free vibration of axially functionally graded Timoshenko beams with non-uniform cross-section, Compos Part B: Eng 45:1493–98.

Li, X.F., Kang, Y.A., Wu, J.X. (2013). Exact frequency equations of free vibration of exponentially functionally graded beams, Appl Acoust 74:413–20.

Liu, P., Lin, K., Liu, H., Qin, R. (2016). Free transverse vibration analysis of axially functionally graded tapered Euler-Bernoulli beams through spline finite point method, Shock Vib 2016: Article ID 5891030, 23 pages.

Murin, J., Aminbaghai, M., Hrabovsky, J., Kutis, V., Paulech, J., Kugler, S. (2014). A new 3D FGM beam finite element for modal analysis, Proceedings of the 11th world congress on computational mechanics (WCCM XI), 5th European conference on computational mechanics (ECCM V), 6th European conference on computational fluid dynamics (ECFD VI). Barcelona, Spain.

Murin, J., Aminbaghai, M., Hrabovsky, J., Kutis, V., Paulech, J., Kugler, S. (2016). Beam finite element for modal analysis of FGM structures, Engineering Structures 121:1-18.

Murin, J., Aminbaghai, M., Kutis, V. (2010). Exact solution of the bending vibration problem of FGM beams with variation of material properties, Eng Struct 32:1631-40.

Natarajon, S., Baiz, P.M., Bordas, S., Rabczuk, T., Kerfriden, P. (2011). Natural frequencies of cracked functionally graded material plates by the extended finite element method, Compos Struct 93:3082-92.

Nguyen, T.K., Vo, T.P., Thai, H.T. (2013). Static and free vibration of axially loaded functionally graded beams based on the first-order shear deformation theory, Compos Part B: Eng 55:147–57.

Pradhan, K., Chakraverty, S. (2014). Effects of different shear deformation theories on free vibration of functionally graded beams, Int J Mech Sci 82:149-60.

Rajasekaran, S. (2013a), Differential transformation and differential quadrature methods for centrifugally stiffened axially functionally graded tapered beams, Int J Mech Sci 74 :15–31.

Rajasekaran, S. (2013b). Free vibration of centrifugally stiffened axially functionally graded tapered Timoshenko beams using differential transformation and quadrature methods, Appl Math Mod 37:4440–63.

Sarkar, K., Ganguli, R. (2014). Closed-form solutions for axially functionally graded Timoshenko beams having uniform cross-section and fixed–fixed boundary condition, Compos Part B: Eng 58:361–70.

Shahba, A., Attarnejad, R., Marvi, M.T., Hajilar, S. (2011). Free vibration and stability analysis of axially functionally graded tapered Timoshenko beams with classic and non-classical boundary conditions, Compos Part B: Eng 42:801-08.

Shahba, A., Rajasekaran, S. (2012). Free vibration and stability of tapered Euler–Bernoulli beams made of axially functionally graded materials, Appl Math Mod 36:3094–111.

Simsek, M. (2010). Vibration analysis of a functionally graded beam under a moving mass by using different beam theories, Compos Struct 92:904-17.

Su, H., Banerjee, J.R. (2015). Development of dynamic stiffness method for free vibration of functionally graded Timoshenko beams, Comput Struct 147:107–16.

Sun, D.L., Li, L.F. (2019.) Initial value method for free vibration of axially loaded functionally graded Timoshenko beams with nonuniform cross section, Mech Based Des Struct Mach 47:102-20.

Tang, A.Y., Wu, J.X., Li, X.F., Lee, K.Y. (2014). Exact frequency equations of free vibration of exponentially non-uniform functionally graded Timoshenko beams, Int J Mech Sci 89: 1–11.

Thai, H.T., Vo, T.P. (2012). Bending and free vibration of functionally graded beams using various higher-order shear deformation beam theories. Int J Mech Sci 62:57–66.

Trefethen L.N., (2000). Spectral Methods in MATLAB, Software, Environments, and Tools, SIAM (Philadelphia).

Wattanasakulpong, N., Mao, Q. (2015). Dynamic response of Timoshenko functionally graded beams with classical and non-classical boundary conditions using Chebyshev collocation method, Compos Struct 119:346–54.

Zhao, Y., Huang, Y., Guo, M. (2017). A novel approach for free vibration of axially functionally graded beams with non-uniform cross-section based on Chebyshev polynomials theory, Compos Struct 168:277-84.